frontiers in Environmental Science

ORIGINAL RESEARCH
published: 05 April 2019
doi: 10.3389/fenvs.2019.00040

Riparian Vegetation and Sediment Supply Regulate the Morphodynamic Response of an Experimental Stream to Floods

Anne F. Lightbody[1]*, *Li Kui*[2,3], *John C. Stella*[2], *Krysia W. Skorko*[1], *Sharon Bywater-Reyes*[4,5] and *Andrew C. Wilcox*[4]

[1] Department of Earth Sciences, University of New Hampshire, Durham, NH, United States, [2] Department of Forest and Natural Resources Management, College of Environmental Science and Forestry, State University of New York, Syracuse, NY, United States, [3] Marine Science Institute, University of California, Santa Barbara, Santa Barbara, CA, United States, [4] Department of Geosciences, University of Montana, Missoula, MT, United States, [5] Department of Earth and Atmospheric Sciences, University of Northern Colorado, Greeley, CO, United States

Feedbacks between woody plants and fluvial morphodynamics result in co-development of riparian vegetation communities and channel form. To advance mechanistic knowledge regarding these interactions, we measured the response of topography and flow to the presence of riparian tree seedlings with contrasting morphologies in an experimental, field-scale, meandering stream channel with a mobile sand bed. On a convex point bar, we installed seedlings of *Tamarix* spp. (tamarisk) and *Populus fremontii* (cottonwood) with intact roots and simulated a bankfull flood, with each of eight runs varying sediment supply, plant density, and plant species. Vegetation reduced turbulence and velocities on the bar relative to bare-bed conditions, inducing sediment deposition when vegetation was present, regardless of vegetation density or species. Sediment supply also played a dominant role, and eliminating sediment supply reduced deposition regardless of the presence of vegetation. Unexpectedly, plant density and species architecture (shrubby tamarisk vs. single-stemmed cottonwood) had only a secondary influence on hydraulics and sediment transport. In the absence of plants, mobile bedforms were prominent across the bar, but vegetation of all types decreased the height and lateral extent of bedforms migrating across the bar, suggesting a mechanism by which vegetation modulates feedbacks among sediment transport, topography, and hydraulics. Our measurements and resulting insights bridge the gap between laboratory conditions and real dryland sand-bed rivers and motivate further morphodynamic modeling.

Keywords: ecogeomorphology, ecohydraulics, morphodynamics, fluvial geomorphology, plant ecology, riparian vegetation, sediment transport, sediment supply

OPEN ACCESS

Edited by:
Paolo Perona, University of Edinburgh, United Kingdom

Reviewed by:
Eric Josef Ribeiro Parteli, Universität zu Köln, Germany
Renan De Souza Rezende, Regional Community University of Chapecó, Brazil

***Correspondence:**
Anne F. Lightbody
anne.lightbody@unh.edu

Specialty section:
This article was submitted to Freshwater Science, a section of the journal Frontiers in Environmental Science

Received: *02 October 2018*
Accepted: *13 March 2019*
Published: *05 April 2019*

Citation:
Lightbody AF, Kui L, Stella JC, Skorko KW, Bywater-Reyes S and Wilcox AC (2019) Riparian Vegetation and Sediment Supply Regulate the Morphodynamic Response of an Experimental Stream to Floods. Front. Environ. Sci. 7:40. doi: 10.3389/fenvs.2019.00040

INTRODUCTION

Interacting physical and biological processes in river-floodplain systems shape ecosystems and channels (Naiman and Decamps, 1997; Gurnell, 2014; Politti et al., 2018). Vegetation influences hydraulics, sediment erosion and deposition (López and García, 1998; Neumeier and Ciavola, 2004; Bouma et al., 2007; Nepf, 2012; Manners et al., 2015), and channel morphology

(Gran and Paola, 2001; Simon and Collison, 2002). For example, bank stabilization by vegetation can influence meander migration, foster single-thread channels, reduce braiding, and reduce channel width (Williams, 1978; Gran and Paola, 2001; Micheli and Kirchner, 2002; Simon and Collison, 2002; Allmendinger et al., 2005; Tal and Paola, 2007). Similarly, flood and sedimentation history influence plant mortality (Wilcox and Shafroth, 2013; Bywater-Reyes et al., 2015), the cohort structure of riparian tree populations, and the successional trajectory of vegetation communities (Scott et al., 1996; Balian and Naiman, 2005; Birken and Cooper, 2006; Stella et al., 2011).

Feedbacks between vegetation and morphodynamics impact the ecology and management of riparian zones worldwide. For example, along dryland rivers in the southwestern U.S. (Merritt and Poff, 2010), widespread invasion by the non-native shrub tamarisk (or saltcedar, *Tamarix* spp.) has replaced native tree communities of willow (*Salix gooddingii*) and cottonwood (*Populus fremontii*) (Di Tomaso, 1998; Stromberg et al., 2007). Tamarisk management has in some cases had unintended geomorphic consequences: for example, on the Rio Puerco, NM, herbicide application to kill tamarisk reduced its cohesive effect, after which flooding caused extensive erosion and channel enlargement (Vincent et al., 2009; Griffin et al., 2014). Because the dispersal (Stella et al., 2006), growth characteristics (Mahoney and Rood, 1998), and other life history traits of cottonwood and willow are adapted to disturbance, these species are typically the first woody plants to colonize riparian areas following disturbances (Braatne et al., 1996; Karrenberg et al., 2002). Cottonwood trees in particular have high ecological value (Rood et al., 2005) as well as sensitivity to altered flow regimes (Rood et al., 2003a; Stella et al., 2010); maintaining cottonwood is thus a management objective along many rivers in its native range (Rood et al., 2003b). But the spread of cottonwood can also pose management challenges: for example, cottonwood (*Populus deltoides*) encroachment following damming along the Platte River, NE has been countered by active tree clearing in an attempt to restore open channel habitat for migratory birds along the formerly wide, shallow braided river (Johnson, 1994; Platte River Recovery Implementation Program, 2006).

Tamarisk and cottonwood produce strong feedbacks with fluvial processes and have distinct interactions with morphodynamics (Kui et al., 2014; Manners et al., 2015; Bywater-Reyes et al., 2017; Diehl et al., 2017a,b). The distribution of tamarisk and cottonwood along rivers thus has not only ecological but also hydrogeomorphic significance. Tamarisk and cottonwood have different ecological-response traits, which reflect adaptations to water availability and fluvial disturbance (Merritt, 2013), and morphological-effect traits that influence flow, sediment transport, and landform stabilization on the basis of their architecture (Kui et al., 2014; Bywater-Reyes et al., 2017; Diehl et al., 2017a). Diehl et al. (2017a) documented ecogeomorphic feedbacks in sand-bed rivers that were mediated by plant-trait differences, showing that flexible stemmed plants (e.g., cottonwood) promoted erosion during floods, whereas more rigid shrubs (e.g., tamarisk) fostered aggradation; in turn, the distribution of plant guilds with similar traits corresponded to abiotic conditions. On the Bill Williams River, Arizona, during five decades of flow regulation and plant encroachment, tamarisk-dominated reaches showed greater channel narrowing and simplification to single-thread form than reaches with native (cottonwood-willow) woodlands (Kui et al., 2017). These field-scale effects have also been documented in flume studies showing differences in tamarisk versus cottonwood effects on hydraulics, sediment deposition and scour patterns (Kui et al., 2014; Diehl et al., 2017b).

Recent advances regarding the influence of vegetation on hydraulics have provided insights on spatial variability in those relationships, shear-stress partitioning, and morphodynamic effects. During flooding, woody plants' stems and leaves influence hydraulics by increasing turbulence (Nepf, 1999), reducing flow velocity and increasing drag within vegetation patches, and increasing velocity outside of patches (Green, 2005; Lightbody et al., 2008; Wilson et al., 2008; Luhar and Nepf, 2012; Yager and Schmeeckle, 2013). Shear layers generated at the boundaries of the flow and individual plants or patches create stem-, patch-, and canopy-scale coherent flow structures (Nepf et al., 2013). Thus, vegetation reduces excess shear stress and consequently may increase fine-sediment deposition and reduce coarse bed-material transport (Larsen et al., 2009; Yager and Schmeeckle, 2013). For example, more abundant vegetation can increase sediment deposition within reaches (Tal and Paola, 2007) and produce reach-average narrowing or aggradation (Williams, 1978; Hopkinson and Wynn, 2009; Griffin et al., 2014). Even though reach-scale deposition may increase, however, individual plant patches may become smaller as a result of increased scour at the edges (Rominger et al., 2010; Dean and Schmidt, 2011), though only if vegetation is sufficiently dense (Hopkinson and Wynn, 2009). At the scale of individual stems, Yager and Schmeeckle (2013) found in a flume study that the introduction of vertical rigid cylinders into a sand-bedded flume disrupted the formation of migrating sand bedforms and instead anchored depositional, non-migrating bedforms and scour holes adjacent to each cylinder. Sediment supply modulates the effect of vegetation on morphodynamics: experiments in a straight flume with live woody seedlings showed that aggradation and erosion reflect a combination of biotic (plant species and configuration) and abiotic (flow rate) drivers under sediment-equilibrium conditions, whereas under sediment-deficit conditions, abiotic factors dampen the effect of variations in plant characteristics on morphodynamic responses (Manners et al., 2015; Diehl et al., 2017b).

Although laboratory studies have advanced the mechanistic understanding of local-scale interactions among plants, hydraulics, and sediment transport, gaps still persist between flume-derived insights and real rivers. For example, measurements of detailed flow fields and morphological response within real vegetation in meandering channels are lacking. Progress in physical modeling of plant-morphodynamic feedbacks could improve representation of vegetation in models of channel planform and landscape development (Istanbulluoglu and Bras, 2005; Beechie et al., 2006; Perucca et al., 2007; Gran et al., 2015) and hydraulic models (Kean and Smith, 2004; Griffin et al., 2005; Wu et al., 2005; Iwasaki et al., 2016). More generally, modeling feedbacks among flow, vegetation, and sediment

remains one of the most complex problems in fluvial hydraulics (Hardy, 2006; Solari et al., 2016).

In this context, we designed an experimental study to measure the influence of young woody plants on bar-bend morphodynamics in a sand-bed channel in order to understand the conditions of the pioneer phase of riparian-woodland development, in which plants such as tamarisk, cottonwood, and willow colonize newly created bars and banks (Mahoney and Rood, 1998; Bendix and Stella, 2013). Previous work (as cited above) highlights the potential for strong ecogeomorphic feedbacks in these systems. Because floods in sand-bed rivers typically exceed thresholds for bed mobility [i.e., "live bed" (Henderson, 1963) or "labile" (Church, 2006) streams], and exist in the transition between the laminar and turbulent boundary layer regimes (Charru et al., 2013), the morphology of bedforms, bars and channels can be highly dynamic. Therefore, the time scales for channel change and vegetation change in these systems may be similar.

In this study, we installed live seedlings of tamarisk (*Tamarix* spp.) and cottonwood (*Populus fremontii*) with intact root systems into a sand-bedded, meandering, field-scale experimental channel at different densities and species configurations to document how these vegetation attributes affect channel sediment dynamics and flow. The study comprised a series of trials that imposed flows simulating a bankfull flood under contrasting equilibrium and deficit sediment supply and with various plant-patch configurations. More specifically, we sought to understand how woody seedlings with shrubby (i.e., tamarisk) vs. tree-like (i.e., cottonwood) architecture, at high and low field densities and in monospecific vs. mixed patches, would influence topographic evolution and flow hydraulics across a meander bend during flood conditions. We measured several responses including bedform development and migration, bed-elevation change, flow velocity fields, and turbulence. This experimental approach was novel in its measurement of morphodynamic responses to pioneer riparian vegetation and sediment-supply variability in a flume that bridges the gap between laboratory conditions and field settings representative of dryland sand-bed rivers.

METHODS

Experimental Facility and Runs

Experiments were conducted at the University of Minnesota St. Anthony Falls Laboratory Outdoor StreamLab. This experimental facility (**Figure 1**) was configured into a flat floodplain bisected by a meandering sand-bed stream channel that was 50 m long with bankfull width 3 m, average bankfull depth 0.3 m, and sinuosity (channel length / valley length) of 1.3. The channel consisted of three bends, the lower two of which each contained a central self-built point bar accreted as a result of sediment transported in the stream. Streamside vegetation, coir logs, and coconut fiber matting provided bank stabilization within the entire stream channel, and two constructed riffles formed from larger immobile cobble were located in the crossings between each bend. The bed sediment was coarse sand with a median grain size of 0.7 mm ($d_{16} = 0.35$ mm, $d_{84} = 1.2$ mm).

The unique field-scale OSL facility allowed control of sediment and water supply entering the reach. Sediment supply was controlled by an adjustable sediment feeder at the stream inlet. Approximately once per hour, the amount of sediment exiting the feeder during a 2-min interval was collected, dried, and weighed. Sediment transported out of the downstream end of the channel was captured in a large stilling basin, surveyed for volume estimation, subsampled for bulk density determination, and then recirculated for later feed.

We conducted eight runs during steady water discharge under either equilibrium sediment supply (Runs 0–4) or no sediment supply (Runs 5–7; i.e., sediment-deficit conditions) to test how hydraulic factors and sediment transport were affected by variation in plant density, species, and sediment supply (**Table 1**). The first (Run 0) and last (Run 7) experimental runs consisted of a bare channel bed (no vegetation) as a control. After Run 0, we installed plants on the portion of the sand bar in the middle meander bend exposed at low flow, and we used the Run 0 final bar elevation for grading the bar surface prior to all runs. The reinstallation of plants and the regrading of the bar before each run eliminated spatial autocorrelation between trials. We used live tamarisk (*Tamarix* spp.) and cottonwood (*Populus fremontii*) seedlings, which had been harvested from the Bill Williams River, AZ, replanted into sediment extracted from the experimental facility, and placed in portable plant propagation pots (30 cm diameter by 30 cm deep) with removable side panels (**Figure 1**). At the beginning of Runs 1–4 and Run 6, we installed 43 pots containing a combination of cottonwood and tamarisk seedlings at sparse (2 plants per pot, or 24 plants m^{-2}) or dense (17 plants per pot, or 240 plants m^{-2}) spacing rooted in flume bed sediment (**Figure S1**). Because Run 4 did not result in substantial plant damage or loss, we used the vegetation that survived Run 4 in Run 5. The sides of the pots were removed prior to flooding and gaps between pots were backfilled with loose sediment to create a point bar composed of continuous mobile sediment with rooted seedlings.

Following vegetation installation for each run, we raised discharge over a period of ∼5 min to constant bankfull flood conditions (discharge of 283 ± 4 L s^{-1}) to inundate all seedlings, and held that rate for at least 6 h. During Runs 1–4, sediment was fed at a rate of 7 ± 1 kg/min of dry sediment equivalent; during Runs 5–7, no new sediment was fed (**Figure S2**). All runs began with an equilibration period during which water and sediment flux were allowed to stabilize. Equilibrium conditions were considered to occur when repeated cross-section topographic measurements (see below) revealed a steady bar volume in the middle meander bend. The first run during each sediment supply condition required a greater time for topographic adjustment: Run 0 (first equilibrium supply run) required 17 h and Run 5 (first deficit supply run) required 13 h, whereas Runs 1–4 (subsequent equilibrium supply runs) each required 2.5 h and Run 6–7 required 2.25 h (**Figure S3**). Nearly all seedlings became fully submerged below the water surface within the first few minutes of each flood and remained rooted in place for the duration, with low mortality due to scour. After each experimental flood

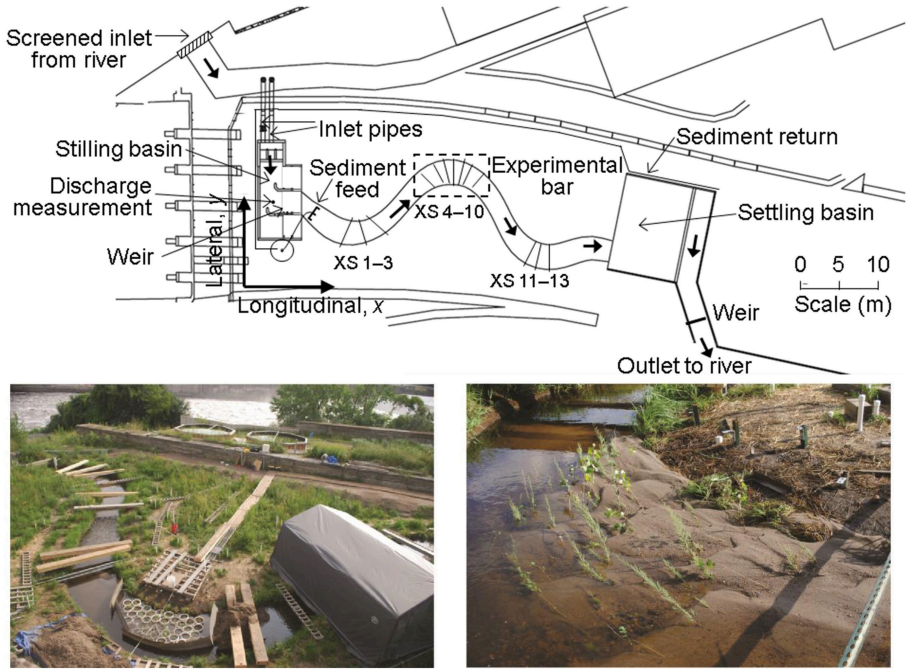

FIGURE 1 | Outdoor StreamLab experimental facility, University of Minnesota. Top shows plan view schematic, where thick arrows indicate water flow from left to right, and fixed locations for cross-section measurements are also shown. Measurement cross-sections were numbered consecutively from upstream to downstream, with cross-sections (XS) 1–3 in the upstream bend, 4–10 in the middle experimental bend, and 11–13 in the downstream bend. Bottom left photo shows the preparation of the study bar along middle meander bend, with pots of propagated plants prior to removing their sides. Flow is from right to left, with the Mississippi River in background. Bottom right photo shows post-flood condition with mixed cottonwood and tamarisk seedlings on the middle meander bend. Top panel reproduced (with modifications) from Kui et al. (2014), with permission of John Wiley and Sons (24 October 2018).

concluded, sediment feed ceased, and stream flow was reduced to base flow levels over a period of ∼15 min. Bar topography did not visibly change during flow recession, although it is possible that some fine-scale features were altered.

Topography Measurements and Analysis

We measured topography using both point measurements during each flood and high-resolution laser and ultrasonic scans following the conclusion of each flood. Topographic measurements were converted to a Cartesian coordinate system used at the OSL facility, with origin at upstream river right (**Figure 1**) and elevation referenced to sea level, using a set of fixed reflectorless benchmarks distributed around the facility and a reflectorless total station (Sokkia X30RK) located on a permanent stationary post.

During each flume run, we performed repeat measurements of bed elevation along fixed cross sections using a manual point gage with sand foot. On each of 13 fixed cross sections, situated orthogonal to flow in all three channel bends (**Figure 1**), the bed elevation was recorded at 10-cm intervals from a horizontal channel-spanning crossbeam. We emphasized rapid, frequent topography measurements along five cross sections in the middle bend, both before and after equilibrium was reached during each run, to account for topographic evolution due to bed form migration, as explained further below.

The point measurements were complemented by scans to produce a high-resolution spatial snapshot of the middle-bend bar surface, obtained immediately following the conclusion of each flood under low base flow conditions when no sand transport was present. These scans were conducted using a high-resolution data acquisition carriage designed for outdoor use that enabled the precise positioning of instrumentation within a 3 m by 1.5 m area of the channel. Subaqueous bathymetry in the bend thalweg was obtained using a Panametrics C304 downward-looking ultrasonic transducer at 1 cm spacing; subaerial topography on the bar surface was obtained using a Keyence laser range finder at 5-mm spacing.

For each run, we computed the time-averaged bar-surface topography for the vegetated middle meander bend. Topography was time averaged in order to integrate the mean effect of each treatment without excess influence by any transient bedform configuration resulting from the presence of migrating bedforms. The time-averaged digital elevation model (DEM) for each run was computed by averaging repeat topography measurements from the five cross-sections centered on the vegetated bar during the sediment equilibrium period, and these values were then spatially interpolated within the streamwise coordinate system. Comparison of the time-averaged topography and the spatially detailed scan snapshot following each run, averaged over the bar surface (e.g., the vegetated polygon shown in **Figure 2**), indicated that the bed elevation at the moment at

TABLE 1 | Vegetation and sediment supply conditions, and measured topographic change and turbulence, for experimental flood runs.

Run number	Plant species	Patch configuration	Cottonwood density (stems m^{-2})[a]	Tamarisk density (stems m^{-2})[a]	Sediment supply	Net topographic change (cm)[b]	Turbulence (m s^{-1})[c]
Run 0	Bare bed	NA	0	0	Equilibrium[d]	NA	0.11 ± 0.04
Run 1	Cottonwood	Dense	240	0	Equilibrium[e]	2.39 ± 3.52*[f]	0.11 ± 0.03
Run 2	Tamarisk	Dense	0	240	Equilibrium[e]	2.96 ± 3.61*	0.12 ± 0.03
Run 3	Mixed	Sparse	12	12	Equilibrium[e]	2.08 ± 1.89*	0.11 ± 0.03
Run 4	Mixed	Dense	120	120	Equilibrium[e]	3.38 ± 3.75*	0.11 ± 0.03
Run 5	Mixed	Dense	115	120	None	0.68 ± 4.95	0.09 ± 0.03*
Run 6	Mixed	Sparse	12	12	None	−0.42 ± 3.30	0.09 ± 0.02*
Run 7	Bare bed	NA	0	0	None	−1.53 ± 1.78*	0.08 ± 0.02*

[a] *Seedling densities are reported as number of stems per unit point bar surface area.*
[b] *Net change was calculated as the difference between the bed surface during the treatment trials (Runs 1–7) and the unvegetated condition (Run 0), in all cases averaging the measurements in each unique location along the unistrut cross sections during each trial. Negative and positive values indicate net scour and deposition, respectively, relative to the unvegetated bar, and are reported as mean ± standard deviation.*
[c] *Turbulence (root mean square of longitudinal velocity) measured in each experimental trial, reported as mean ± standard deviation.*
[d] *Feed rate of 5.3 ± 2.5 kg/min of dry sediment equivalent (Run 0).*
[e] *Feed rate of 7 ± 1 kg min-1 of dry sediment equivalent (Runs 1–4).*
[f] *Asterisks indicate a significant difference from the bare-bed run (Run 0) at equilibrium sediment supply, as indicated in the linear mixed model and pairwise Tukey HSD tests (**Table S1** for net topographic change and **Table S3** for turbulence).*

which the flood was stopped (i.e., as measured by the scan snapshot) was indistinguishable from the bed elevation at other times during the flood, as represented by the time-averaged topography (**Figures S4**, **S5**).

To explore topographic change associated with different vegetation attributes and sediment supply conditions, we statistically compared the time-averaged bed elevation during each run along the cross sections in the middle bend (**Figure 1**). For each cross section, all point and scan measurements were linearly interpolated to common locations. The point measurements were taken ≥25 cm apart, which exceeded the dimensions of transient bedforms; therefore we considered these bed measurement locations spatially independent. For each run, all repeat measurements at each location were averaged, thus avoiding temporal pseudoreplication.

First, we compared each run to the bare-bed trial at equilibrium sediment supply (Run 0) to assess net changes from the reference condition. Next we subtracted the time-averaged elevations of the treatment runs from the corresponding reference elevations (Run 0) and compared the elevation differences among treatments using a mixed linear model with the runs as the categorical fixed factor and cross section as a random variable. We compared pairwise differences between runs using Tukey's honest significant difference (HSD) *post-hoc* test, which adjusts the threshold significance value for the number of tests performed.

In addition, as a measure of the intensity of bedform migration, we calculated the standard deviation of repeat bed-elevation values measured at the same locations at different times during active bedform migration. We interpolated these values into geospatial response surfaces to visualize the relative intensity of bedform movement across the bar surface.

Velocity Measurements and Analysis

During equilibrium conditions, we measured the three-dimensional velocity field in the middle meander bend using a Nortek Vectrino acoustic Doppler velocimeter (ADV). The downward-looking probe was suspended from a traversing mount that spanned the width of the channel. Point measurements were obtained along two cross sections: just upstream of the vegetated region (cross section Conclusion) and at the apex of the vegetated bar (cross section 7). Across each cross section, we measured at approximately 20 locations (5–6 verticals at ∼30 cm lateral spacing, with 2–4 locations on each vertical) over a time period of ∼2 h; measurements were more complete on cross section 7 than on cross section Conclusion. The velocity at each point was measured at 200 Hz for 3 min, which was long enough to observe convergence of both mean velocity and turbulence statistics. During vegetated runs, we modified the lateral spacing of measurements to prevent vegetation from interfering with the probe sampling volume.

Velocity data were post-processed using WinADV32 v.2.029 (Bureau of Reclamation), using phase-space threshold despiking and discarding data points with communication errors, minimum correlation value below 40, and minimum signal-to-noise ratio below 10 (Wahl, 2000). As a measure of turbulence, we calculated the root mean square of longitudinal velocity (u_{rms}).

We statistically compared the velocity data between runs in 2 ways. First, we calculated the gradient in longitudinal velocity across the stream from the bar to the thalweg to understand how the velocity distribution depended on plant configuration. In addition, velocity measurements conducted at all locations and depths were compared between runs using analysis of covariance (ANCOVA) with distance across the cross section as a continuous variable and treatments (runs) as a discrete factor. A *post-hoc* paired *t*-test on the velocity gradients was performed to understand how the velocity along the lateral

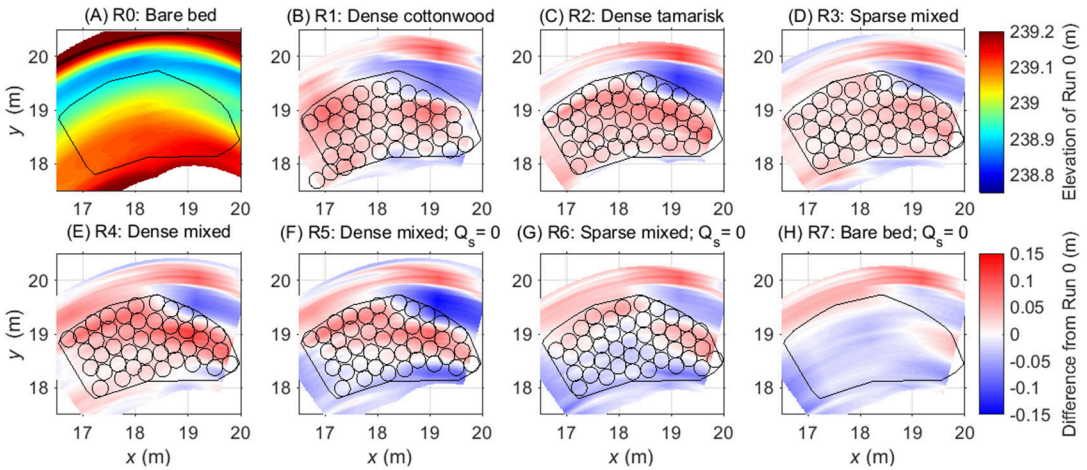

FIGURE 2 | Difference between time-averaged equilibrium topography data for Runs 1–7 and the equilibrium topography observed during the bare-bed, equilibrium sediment supply run **(A)**; color ramp shows time-average elevation), which is shown here to facilitate interpretation of **(B–H)**, which follow color ramp shown at right. Panels **(A–E)** (Runs 0–4) show runs with equilibrium sediment supply; **(F–H)** show runs with no sediment supply ($Q_S = 0$). Black circles show the locations of vegetation pots from each run, and the black polygon indicates the horizontal extent of the region that, in Runs 1–6, contained vegetation. Red shading indicates net deposition over the course of the run. This is especially evident for the dense mixed configuration (Run 4), dense tamarisk (Run 2), and to a lesser degree dense cottonwood (Run 1) and the sparse mixed patch (Run 3). Sediment-deficit conditions (Runs 5–7) largely counteracted the deposition effects of the plants. Distances along x and y axes are relative to the Cartesian coordinate system used at the OSL facility, with origin at upstream river right (**Figure 1**).

profile changes across runs (**Table S2**). Finally, we compared turbulence (u_{rms}) values between runs using a linear mixed model, with lateral location as a random factor and run as a fixed categorical factor.

RESULTS

Reach-Scale Flow and Sediment Dynamics

Averaged across all runs, the water surface slope over the entire stream was 0.0072 ± 0.0001, and the water surface slope across the middle bar was 0.0019 ± 0.0002 (between streamwise coordinates 18–22 m in **Figure 3**). The measurement phase of each experimental run occurred after the middle meander bend had finished topographic adjustment to imposed changes in sediment supply, but the reach as a whole exhibited reach-scale variability in sediment output, and thus sediment storage, among runs. At equilibrium supply (Runs 1–4), more sediment entered than exited the stream, resulting in increased sediment storage within the channel over the course of these trials. Longitudinal profiles indicate that this storage was accommodated by deposition in the pools located immediately upstream of the apex of each bend (**Figure 3**).

Eliminating the sediment supply during Runs 5–7 did not result in an immediate reduction in sediment flux exiting the downstream end of the experimental stream, suggesting continued mobilization of sand stored during the previous runs. In fact, longitudinal profiles (**Figure 3**) showed that bed elevation decreased by up to 30 cm along the outside of meander bends at equilibrium flood conditions during these deficit runs. Specifically, the pool upstream of the apex of the middle meander bend reached its maximum excavated depth by Run 6, but the pool upstream of the apex of the lower meander bend continued to evacuate between Runs 6 and 7, suggesting the progressive downstream depletion of sediment supply. Mass balance calculations indicated that the change in sediment storage in the stream bed was the correct magnitude to supply the sediment flux out of the stream during Runs 5–7 (**Supplementary Material** section Methods), and no sediment transport across the surface of the point bar in the middle meander bend was observed during Runs 6 or 7.

Bar-Scale Topographic Response to Varying Vegetation and Sediment Supply Conditions

The addition of vegetation to the point bar altered bar topography and bedform migration. In comparing the equilibrium time-averaged topography among runs, the elevation of the bar surface increased when vegetation was present (**Figure 2**). This increase in elevation of the bar was balanced by a deepening of the thalweg adjacent to the vegetated bar (**Figure 3**). Some portions of the bar were also prone to scour, including the downstream outer bar edge and upstream inner bar edge (**Figures 2B–E**). For runs with equilibrium sediment supply, the increase in bar-surface elevation induced by vegetation in Runs 1–4 was significant relative to Run 0 in pairwise tests (all Tukey HSD tests, $p < 0.05$; **Table 1**; **Figure 4**). Dense vegetation, particularly when containing tamarisk in monoculture or in mixes, had the highest rates of sediment accretion (**Table 1**); however, differences in topographic change between vegetation types were not statistically significant among runs with equilibrium sediment supply (**Figure 4**).

Sediment-deficit conditions largely counteracted the sediment trapping effects of vegetation (**Figure 4**). When comparing

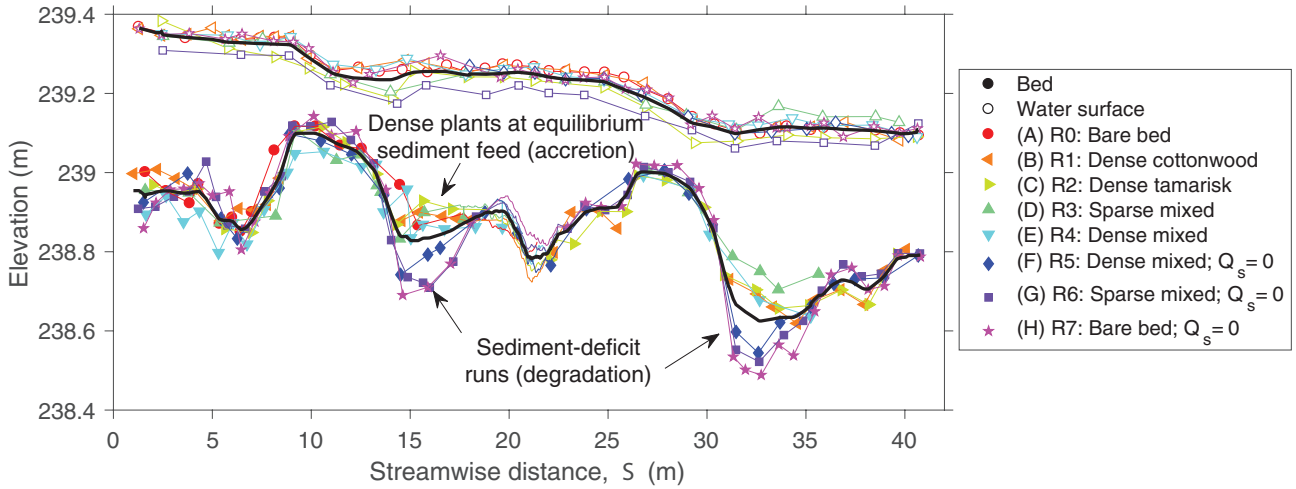

FIGURE 3 | Longitudinal profile of thalweg and water-surface elevation in each experimental run, measured by total station and rod (symbols and thin straight lines) and by scans from data acquisition carriage (thin curved lines for $S = 18$–22 m). Thick black lines show averages across all trials. Riffles were located between streamwise distances of 8–14 m and 25–31 m.

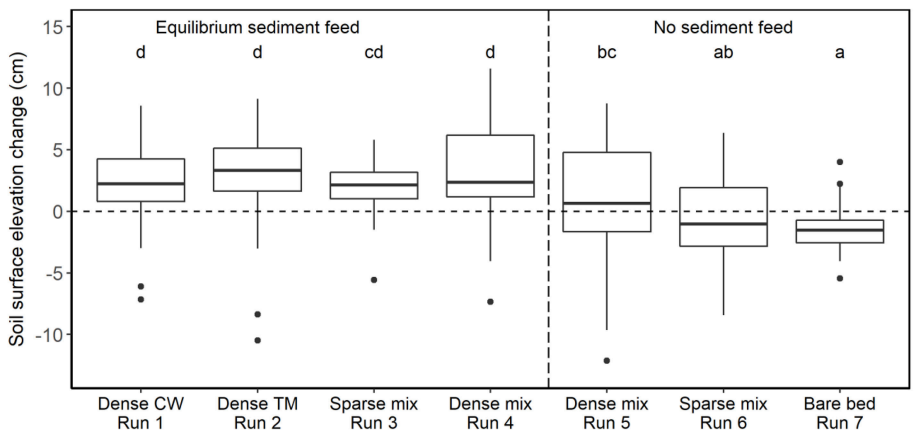

FIGURE 4 | Boxplots of the topographic change induced in each experimental trial relative to the unvegetated bar at equilibrium sediment supply (Run 0). CW denotes cottonwood and TM denotes tamarisk; patch densities are reported in **Table 1**. Repeat measurements at each point along the cross sections were averaged over the course of the run prior to calculating differences from the reference run values, which were also time-averaged to account for transient bedforms. Thick horizontal lines denote median values, box boundaries indicate interquartile range, and whisker heights indicate interquartile range. Letters on top of each box indicate significance level in Tukey's HSD test, which conservatively adjusts the significance threshold based on the number of pairwise contrasts. Under equilibrium sediment transport conditions (boxes left of vertical dashed line), dense tamarisk and dense mixed species induced somewhat higher sedimentation than dense cottonwood or sparse mixed plants. Sediment-deficit conditions (right of vertical dashed line) induced minimal deposition on the vegetated bar, though plant density still had a positive effect on deposition (Run 5 > Run 6). Net erosion occurred during the bare-bed run (no plants) under sediment-deficit conditions (Run 7).

identical configurations of mixed-species patches under equilibrium vs. deficit conditions, reducing the sediment supply induced significantly less deposition for both the dense patches (Runs 4 vs. 5) and the sparse ones (Runs 3 vs. 6; $p < 0.05$, **Table S1**). The trials with no sediment supply and sparse plants (Runs 5 and 6) induced negligible deposition, indicating that sediment deficit counterbalanced the effect of plants. The effect of sediment deficit alone is seen in the response of the bare-bed run (Run 7), which was the only deficit run that experienced significant net erosion (-1.53 ± 1.78 cm) relative to the bare-bed, equilibrium sediment-supply trial (Run 0; $p < 0.05$, **Supplementary Table S1**).

During equilibrium sediment supply with unvegetated conditions (Run 0), transient sand migrating bedforms created large (up to 15 cm amplitude) fluctuations in the instantaneous bar surface even after equilibrium conditions were reached (**Figure 5**). The addition of vegetation to the bar disrupted the formation and passage of large-scale bed features. Temporal variability across the bar was reduced in Runs 1–4 compared to Run 0 (**Figure 6**), and

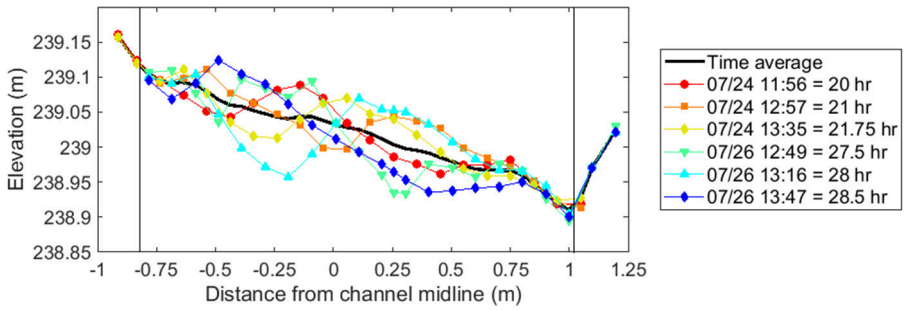

FIGURE 5 | Repeat measurements of topography over 8.5 h on cross-section 10, located at the downstream end of the middle meander bend, during bare-bed, equilibrium sediment-feed conditions (Run 0). These data illustrate the presence of large migrating bedforms, resulting in up to 15 cm vertical bed elevation deviation on the edge of the bar, between repeat surveys. Each measurement is identified by the date and time acquired, as well as the cumulative flood time. The thick black line shows the time-averaged topography at this cross section. Thin vertical black lines indicate the edges of the active sand-bed substrate.

coherent bedforms were less apparent in the post-flood bar topography.

When sediment supply was eliminated (Runs 5–7), net degradation occurred, the bar elevation generally decreased (**Figures 2F–H**, **6**), and the bar surface became armored by the coarsest fraction (pea-gravel size) of the sediment grain size distribution, which the flow was not competent to transport. During these sediment-deficit conditions, temporal fluctuations in the bar surface were undetectable, suggesting an absence of sediment transport across the bar surface via bedforms. Local deposition patterns during sediment-deficit trials (Runs 5–6) instead depended on the location of rooted vegetation.

Velocity and Turbulence Responses

Point measurements collected at two cross sections revealed that longitudinal velocities were significantly faster in the thalweg (0.61 ± 0.019 m s^{-1}) than on top of the bar (0.53 ± 0.016 m s^{-1}), regardless of the presence of vegetation ($t = 4.8$, $p < 0.001$). These general patterns are evident both at the bend apex (cross section 7; **Figure 7**) and upstream of the bar (cross section Conclusion; **Figure S6**). During sediment-equilibrium conditions, dense plants, particularly tamarisk, induced the greatest gradient in longitudinal velocity between bar top and thalweg, whereas velocity distributions were homogenized across the stream for all treatments during sediment-deficit conditions (**Figure 8**). Compared to an unvegetated condition, water velocity on the bar slowed considerably when dense plants were present, while the velocity in the thalweg increased to maintain the same channel discharge. As a result, the velocity gradient across the bar and channel increased, especially for dense tamarisk, and to a lesser extent dense cottonwood, under equilibrium sediment supply. Thus, dense configurations of tamarisk seedlings altered water velocities to a significantly greater degree than cottonwood compared to sparse or no vegetation ($p < 0.05$ for all pairwise contrasts; **Supplementary Table S2**).

Turbulence characteristics also responded to vegetation and sediment supply (**Figure 7**, right column; **Figure 9**). All of the runs had decreased turbulence (indicated by u_{rms}) relative to the reference trial (Run 0), except for the dense tamarisk configuration at equilibrium sediment supply (Run 2), in which turbulence levels were slightly elevated (the linear mixed model coefficients are shown in **Table S3**). However, none of the vegetation trials had significantly different u_{rms}values from the bare-bed, equilibrium sediment-supply run ($p > 0.05$; **Table 1**). In contrast, turbulence decreased substantially when sediment supply was eliminated (pairwise t-test mean effect size = 0.029 m s^{-1}; t =-6.04, p <0.001), likely due in part to the decrease in large-scale bed fluctuations. When controlling for lateral location (i.e., location as a random factor in a linear mixed model), all of the sediment-deficit trials, regardless of plant configuration (Runs 5–7), had significantly lower turbulence than the bare-bed run (linear mixed model, $p \leq 0.05$; **Table 1**; **Figure 9**; **Table S3**).

DISCUSSION

The novel set of experiments reported here, using live woody seedlings in a meandering flume, show the influence of plant density and architecture on hydraulics and sediment transport within a bar-bend sequence during floods simulating bankfull conditions with varying sediment supply. Overall the greatest alterations in sediment deposition, water velocity, and turbulence were induced by the presence of plants and the reduction in sediment supply. Plant density and species architecture (shrubby tamarisk vs. single-stemmed cottonwood) had additional but small effects on these responses. Our measurements and resulting insights bridge the gap between laboratory conditions and field settings representative of dryland sand-bed rivers.

Effects of Plant Characteristics on Sediment Dynamics and Flow

During flood conditions, vegetation promoted deposition on the bar surface, interrupted migrating bedforms, and altered lateral gradients in longitudinal velocity. Dense patches with equilibrium sediment supply promoted the greatest sediment deposition, bar-surface aggradation, and reductions in bedform mobility. Our finding that the presence of vegetation inhibited the passage of migrating bedforms is

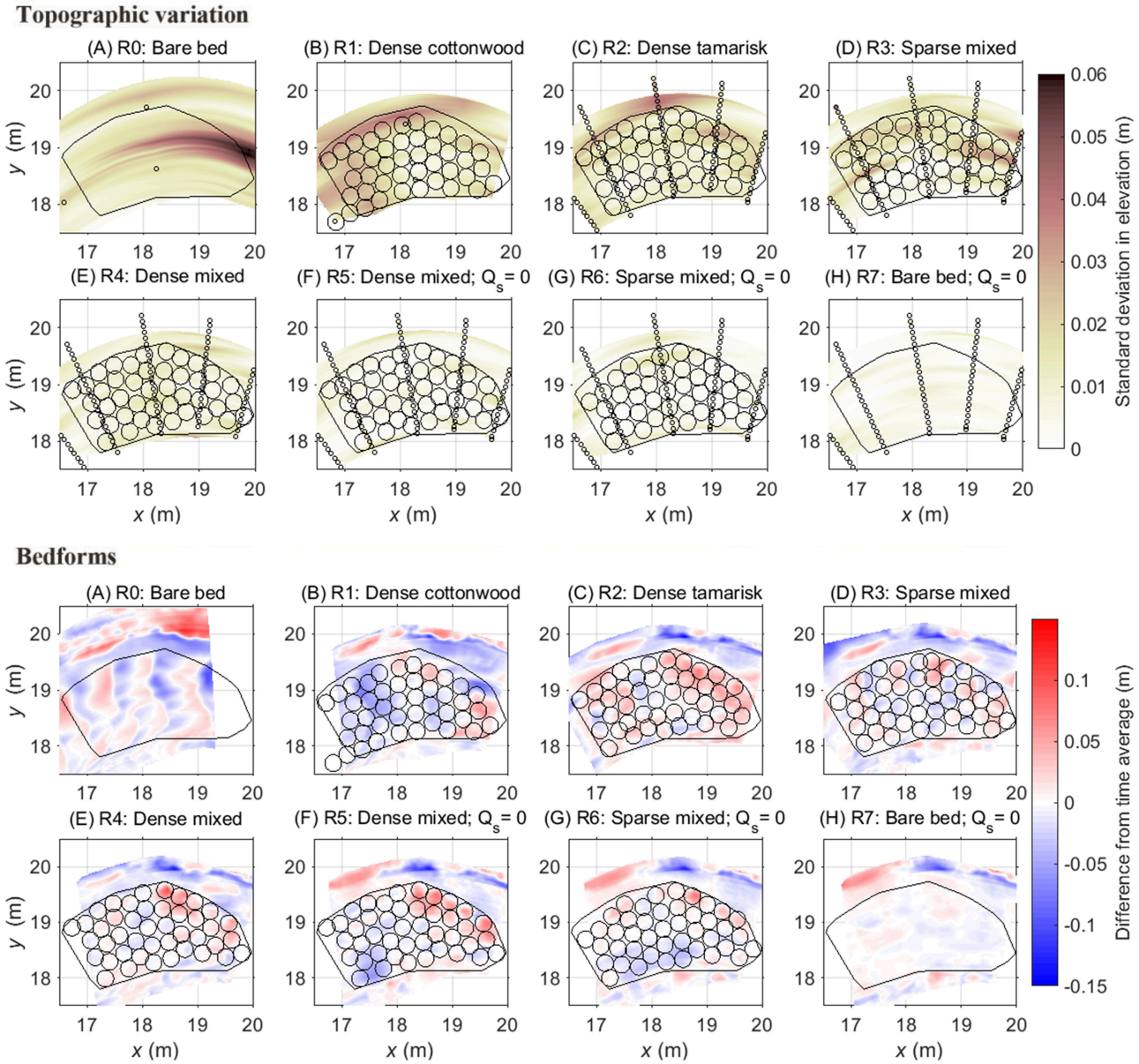

FIGURE 6 | Top panels: topographic variation during the runs as indicated by the standard deviation in elevation among repeated measurements at the same location during equilibrium flood conditions. Black circles show the locations of vegetation pots from each run, and the black polygon indicates the areal extent of the region that, in Runs 1–6, contained vegetation. The stream bed experienced the greatest variation in elevation change during the dense cottonwood (Run 1), dense tamarisk (Run 2) and sparse mixed (Run 3) trials at equilibrium sediment feed. Bottom panels: Evidence of bedforms, as indicated by the difference between scan data, which provide a high-resolution spatial snapshot of bar topography at the end of each run (see **Figure S6**), and time-averaged data during each run (see **Figure S5**). Organized bedforms are evident in the bare-bed trial (Run 0), and to a lesser degree in the dense cottonwood (Run 1), dense tamarisk (Run 2) and sparse mixed (Run 3) runs at equilibrium sediment feed. Bedforms were largely suppressed under sediment-deficit conditions (Runs 5–7) and in the dense mixed trial (Run 4), which had the greatest variation in canopy roughness within the patch. Distances along x and y axes are relative to the Cartesian coordinate system used at the OSL facility, with origin at upstream river right (**Figure 1**).

consistent with experimental studies (Yager and Schmeeckle, 2013) and numerical modeling (Luna et al., 2009) using vegetation proxies; together these results reinforce that vegetation alters sediment-transport dynamics in labile, sand-bed systems.

Our observations indicated that, in addition to stabilizing bars, plants altered velocity fields, complementing previous hydraulic modeling efforts. The morphodynamic behavior of aeolian dunes has also been shown to respond to the height of vegetation cover (Luna et al., 2009), and subaqueous

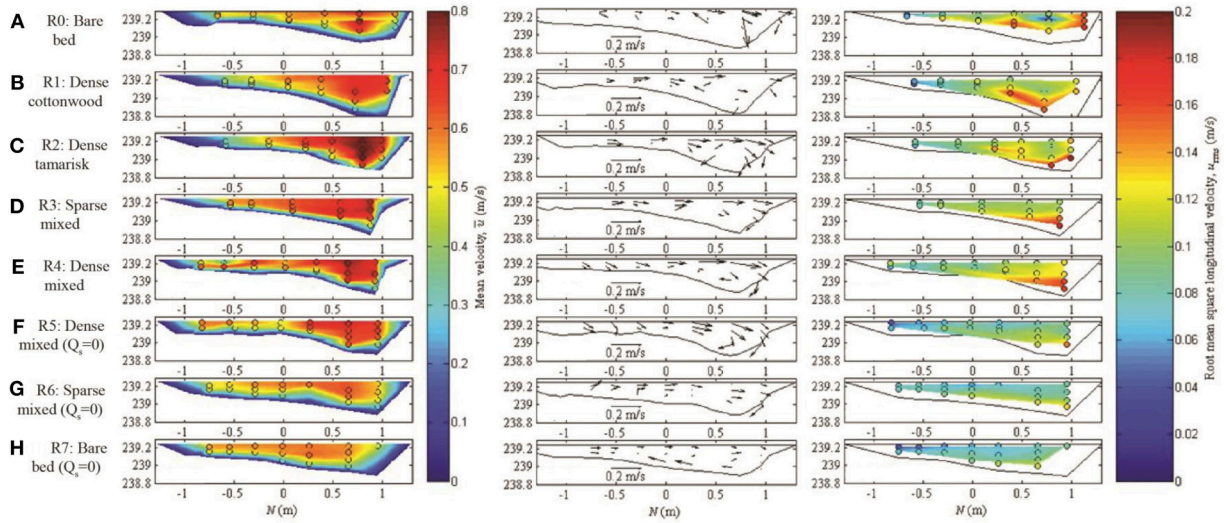

FIGURE 7 | Flow hydraulics for each run at cross section 7, which is at the apex of the middle meander bend, including (left) time-averaged longitudinal velocity; (center) time-averaged lateral and vertical velocity (a scale arrow is located at the bottom of each plot); and (right) root mean square longitudinal velocity, which provides a measure of turbulence. The view is looking upstream; flow is directed out of the page. Vegetation was located at transverse position *N* (x axis) < 0.5 m. In the left and right columns, circles show positions of individual velocity measurements, which are then linearly interpolated between locations and to zero velocity assumed at bed and banks. The dense tamarisk and dense mixed trials (Runs 2 and 4) experienced the greatest velocity reductions within the vegetation patch, with associated amplification of thalweg velocities. Velocity differences between the bar and thalweg were lowest during bare-bed runs with no vegetation (Runs 0 and 7). Under sediment-deficit conditions (Runs 5–7) near-bed turbulence was lower than for equilibrium conditions (right panels).

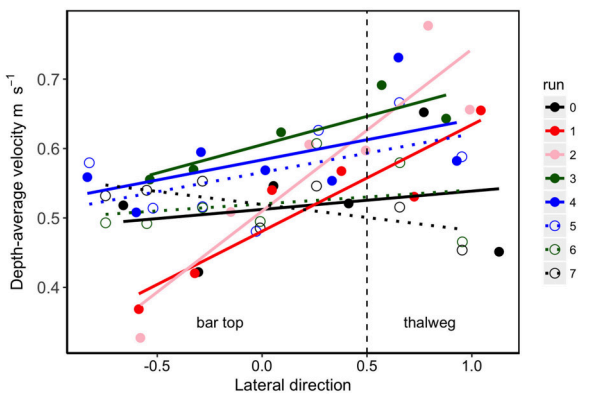

FIGURE 8 | Longitudinal velocity gradient extending from the bar (left) to the thalweg (right) for each run. The vertical dashed line represents the boundary between point bar and channel. Each point represents a depth-average velocity. Steeper slopes indicate slower velocities on the vegetated bar top relative to faster flow in the thalweg. The velocity gradient for the dense tamarisk trial (Run 2) was significantly steeper than the bare bed runs (Runs 0 and 7) and the sediment deficit trial with sparse vegetation (Run 6). In addition, the dense cottonwood trial (Run 1) was significantly different from the bare bed run at sediment deficit (Run 7). Overall these results show that dense plants, particularly tamarisk, induce the greatest alteration in velocity fields when the stream is at equilibrium sediment transport, whereas sediment deficit conditions have the opposite effect of homogenizing the velocity distribution across the stream (**Table S2**).

bedforms behave similarly when they are small relative to the water depth (Charru et al., 2013). A two-dimensional hydraulic model that accounted for vegetation drag in a gravel-bed river (Bywater-Reyes et al., 2018) found patterns of channel-bend hydraulics consistent with those found here. For overbank flows, vegetation caused substantial changes in modeled flow hydraulics compared to an unvegetated bar condition, and addition of dense vegetation to a bar surface resulted in a 30% increase in thalweg velocity and up to 100% reduction of velocities on the bar (Bywater-Reyes et al., 2018). Thus, vegetation-induced changes in velocity and aggradation are countered by corresponding changes in hydraulics and topography in the thalweg, highlighting the potential influence of ecogeomorphic feedbacks on the evolution of meandering rivers.

Though most species-based contrasts in this study were not significant, tamarisk did have a slightly greater effect on morphodynamics (**Figures 4**, **8**, **9**). These differences likely reflect contrasts in these species' morphological-effect traits (Diehl et al., 2017a), and in turn the distinct turbulent structures expected to occur around these plants. Tamarisk seedlings have thicker, more rigid, and more multiple stems than cottonwood, as well as less foliage high on the plant (**Table 2**), such that tamarisk pronate less than cottonwood and induce greater aggradation rates, as observed not only here but also in a set of experiments we completed in a smaller, straight flume (Kui et al., 2014, 2019; Diehl et al., 2017b). The high turbulence (u_{rms}) values associated with cottonwood (Run 1) would be expected to promote sediment suspension and thus limit deposition, analogous to the behavior of sparse cylinders in flume trials (Vargas-Luna et al., 2016). Additionally, the flexibility of cottonwood stems (Kui et al., 2014) may have focused stem-scale turbulence on the bed surface, also inhibiting deposition (Ortiz et al., 2013). The relatively muted effects of species architecture on sediment

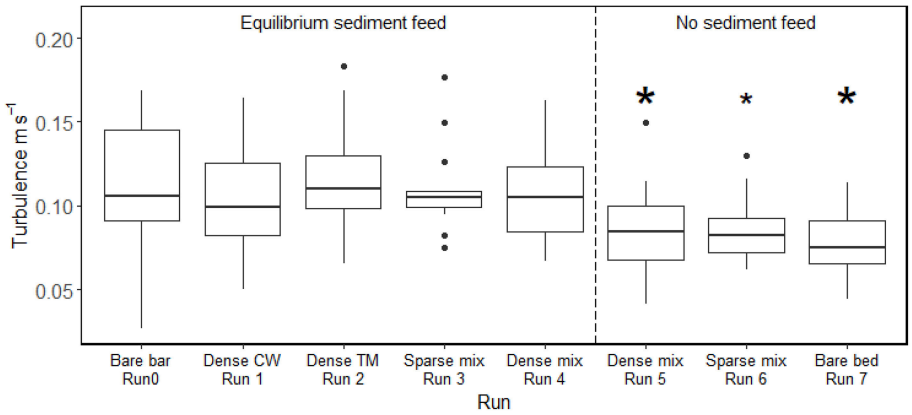

FIGURE 9 | Boxplots of the turbulence (root mean square of longitudinal velocity) induced in each experimental trial. CW denotes cottonwood and TM denotes tamarisk. Thick horizontal lines denote median values, and box boundaries indicate interquartile range. Asterisks on top of each box indicate significant difference compared to the vegetated bar at equilibrium sediment supply (Run 0); the small asterisk for Run 6 indicates a marginally significant difference. The vertical dashed line separates trials with equilibrium sediment transport conditions (left) vs. sediment deficit (right). Only the change in sediment supply induced significant changes in turbulence from the reference condition; none of the plant configurations significantly alter turbulence conditions when sediment supply was taken into account. Details of the statistical tests are reported in **Table S3**.

TABLE 2 | Comparison of plant morphological characteristics (mean ± SD) between cottonwood and tamarisk seedlings, measured from a randomly-selected subset of plants used in the experiment.

Morphological trait	Cottonwood ($n = 53$)	Tamarisk ($n = 40$)
Aboveground height (cm)	30.94 ± 11.12	28.51 ± 14.11
Root length (cm)	19.53 ± 7.81	20.86 ± 9.70
Frontal area (cm^2)	32.25 ± 30.00	42.96 ± 32.71
Stem flexibility (cm cm^{-1})	0.60 ± 0.30	0.50 ± 0.22
Vertical location of maximum crown density (cm)	17.95 ± 13.70	8.45 ± 9.98

deposition and hydraulics in the present study, compared to others that found stronger contrasts, may be due to the greater heterogeneity of the sinuous channel and bar environment, relative to most flumes.

Effects of Sediment Supply on Interactions Between Plants and Morphodynamics

Manipulating the sediment supply allowed us to test how both sediment-equilibrium and sediment-deficit conditions interacted with plant configurations to influence morphodynamic response. Sediment-deficit conditions, as may occur downstream of dams, may promote scour or surface coarsening (e.g., Schmidt and Wilcock, 2008), as well as interacting with vegetation effects on morphodynamics. The largest changes in bed elevation we observed were the aggradational responses with dense seedling configurations (single and mixed species) under sediment-equilibrium conditions. The increased deposition effect of the vegetation was counteracted by elimination of sediment supply; comparison of similar plant configurations but different sediment supply conditions showed significantly less deposition under sediment deficit, and net degradation without plants.

These results somewhat differ from those of a related experiment, in which we also investigated vegetation-morphodynamic feedbacks using live seedlings of cottonwood and tamarisk, with variable discharge and sediment supply, but in a smaller (0.6 m width), straight flume (Diehl et al., 2017b). In those experiments, the greatest change in bed elevation occurred under sediment-deficit conditions. Differences in topographic responses between tamarisk and cottonwood were enhanced under sediment-equilibrium conditions (Diehl et al., 2017b), but that enhancement was not detected here. In the study of Diehl et al. (2017b), density was a major predictor of the magnitude of bed elevation change: sparse vegetation induced scour under deficit conditions, whereas dense vegetation induced deposition. Here, sediment-deficit conditions strongly counteracted the increased deposition effect of the vegetation, with little to no sediment deposition when supply was eliminated, regardless of the presence of vegetation. Our experimental observations complement field results from the Colorado River in Grand Canyon, where dam-induced reductions in supply far outweigh any sediment storage effect by vegetation, resulting in net sediment loss despite the widespread invasion by tamarisk in recent decades (Sankey et al., 2015).

A key effect of varying sediment supply is the impact on plant vulnerability to uprooting or burial during floods. In the experiments documented here, transport capacity was limited because the maximum flood we tested was analogous to a bankfull flood, such that plant dislodgment did not occur (Kui et al., 2014). However, Kui et al. (2019) documented a 35% greater risk of plant loss under sediment-deficit and associated bed degradation, compared to equilibrium sediment conditions. Vulnerability to scour also depended on density (plants in sparse patches dislodged five times more frequently than in dense patches) and species (tamarisk seedlings were less vulnerable to scour than cottonwood; Kui et al., 2019). Similarly, field observations have shown that seedling uprooting is facilitated

by scour around the base of plants, which exposes root systems and thus reduces plant resistance to dislodgement (Bywater-Reyes et al., 2015). Plant loss due to burial during floods can also vary depending on plant traits and/or sediment supply. For example, our results presented here reinforce prior findings that tamarisk seedlings had significantly greater risk of being buried by sediment deposition when small compared to cottonwood (Kui and Stella, 2016) or willow (Wilcox and Shafroth, 2013).

An important dimension of fluvial response to varying sediment supply is adjustment of the bed material size; for example via surface coarsening when transport capacity exceeds supply (Dietrich et al., 1989). The size distribution of sediment supply has also been found to influence ecogeomorphic feedbacks in vegetated, meandering rivers (Braudrick et al., 2009). In our experiment, the size distribution of our sediment feed, which was relatively coarse and traveled as bedload, may have influenced some of the observed patterns of topographic change. Fine sediment, which was not captured effectively in the downstream stilling basin and therefore not fed, is often thought to deposit on the downstream end of bars as a result of helical flow that sweeps fines from the center of the channel up onto the downstream portion of bars (e.g., Dietrich and Smith, 1984). Our observations of scour on the downstream outer edge and upstream inner edge of the bar with vegetation present (**Figures 2B–E**) may reflect the absence of fine sediment in our sediment feed. Moreover, at the end of sediment-deficit runs the bar surface was paved by the coarse fraction (pea-gravel size) of the sediment grain size distribution, which the flow was not competent to transport, suggesting that surface coarsening of the bar may have limited the amount of scour.

CONCLUSION

Mechanistic studies of the interactions among vegetation, hydraulics, and morphodynamics, such as the work we present here, are important for informing river management. For example, there is potential to use flow and sediment management to control riparian vegetation, and in particular promote native species (Rood et al., 2003b). Substantial expenditures and management efforts have been targeted at limiting the spread of the species examined here (e.g., Platte River Recovery Implementation Program, 2006; Vincent et al., 2009), and vegetation-induced channel change and expansion of both native and non-native plants in riparian corridors of dammed rivers is globally important. The insights developed here complement other field and modeling results highlighting how vegetation impacts river hydraulics and morphodynamics, in a manner that can be mediated by sediment supply conditions.

Using field-scale studies such as ours to investigate feedbacks between plants and morphodynamics is important for building links between laboratory studies, real rivers, and management, as well as for improving how vegetation is represented in multidimensional flow and sediment transport models. By using an experimental setup that simulates field conditions, with a meandering mobile-bed channel, transplanted live vegetation, and replicated flood events, we narrow the gap between field and experimental studies. Despite field-scale experimental setups such as ours, understanding and simulating ecogeomorphic feedbacks in real rivers remains challenging.

AUTHOR CONTRIBUTIONS

AL conceived of the project, generated funding, carried out the research and data analysis, and wrote the manuscript. LK carried out the research and data analysis, and wrote the manuscript. JS conceived of the project, generated funding, carried out the research and data analysis, and wrote the manuscript. KS carried out the research and data analysis. SB-R contributed to data collection and manuscript writing. AW conceived of the project, generated funding, and wrote the manuscript.

FUNDING

Funding was provided by the National Science Foundation (EAR 1024652) and through the STC program via the National Center for Earth-surface Dynamics (EAR-0120914).

ACKNOWLEDGMENTS

Invaluable technical and administrative help was provided by Patrick Shafroth, Franklin Dekker, John Welsh, Terry Ettinger, James Johnson, Christina Olivieri, Aaron Daley, Erenis Lemus, and other REU students at the SAFL facility, and SAFL staff including Jess Kozarek, Jeff Marr, Chris Ellis, Jim Mullen, and Dick Christopher. We thank two reviewers for comments that greatly improved the manuscript.

SUPPLEMENTARY MATERIAL

The Supplementary Material for this article can be found online at: https://www.frontiersin.org/articles/10.3389/fenvs.2019.00040/full#supplementary-material

REFERENCES

Allmendinger, N. E., Pizzuto, J. E., Potter, N., Johnson, T. E., and Hession, W. C. (2005). The influence of riparian vegetation on stream width, eastern Pennsylvania, USA. *Geol. Soc. Am. Bull.* 117, 229–243. doi: 10.1130/B25447.1

Balian, E. V., and Naiman, R. J. (2005). Abundance and production of riparian trees in the lowland floodplain of the Queets River, Washington. *Ecosystems* 8, 841–861. doi: 10.1007/s10021-005-0043-4

Beechie, T. J., Liermann, M., Pollock, M. M., Baker, S., and Davies, J. (2006). Channel pattern and river-floodplain dynamics in forested mountain river systems. *Geomorphology* 78, 124–141. doi: 10.1016/j.geomorph.2006.01.030

Bendix, J., and Stella, J. C. (2013). "Riparian vegetation and the fluvial environment: a biogeographic perspective," in *Treatise on Geomorphology*, Vol. 12, eds D.R. Butler and C.R, Hupp (San Diego, CA: Academic Press), 53–74. doi: 10.1016/B978-0-12-374739-6.00322-5

Birken, A. S., and Cooper, D. J. (2006). Processes of *Tamarix* invasion and floodplain development along the lower Green River, Utah. *Ecol. Appl.* 16, 1103–1120. doi: 10.1890/1051-0761(2006)016[1103:POTIAF]2.0.CO;2

Bouma, T., Vanduren, L., Temmerman, S., Claverie, T., Blancogarcia, A., Ysebaert, T., et al. (2007). Spatial flow and sedimentation patterns within patches of epibenthic structures: Combining field, flume and modelling experiments. *Continent. Shelf Res.* 27, 1020–1045. doi: 10.1016/j.csr.2005.12.019

Braatne, J. H., Rood, S. B., and Heilman, P. E. (1996). "Life history, ecology, and conservation of riparian cottonwoods in North America," in *Biology of Populus and its Implications for Management and Conservation (Part I)*, eds R. Settler, H. D. Bradshaw, P. E. Heilman, and T. M. Hinckley (Ottawa, ON: NRC Research Press), 57–85.

Braudrick, C. A., Dietrich, W. E., Leverich, G. T., and Sklar, L. S. (2009). Experimental evidence for the conditions necessary to sustain meandering in coarse-bedded rivers. *Proc. Natl. Acad. Sci. U.S.A* 106, 16936–16941. doi: 10.1073/pnas.0909417106

Bywater-Reyes, S., Diehl, R. M., and Wilcox, A. C. (2018). The influence of a vegetated bar on channel-bend flow dynamics. *Earth Surf. Dynam.* 6, 487–503. doi: 10.5194/esurf-6-487-2018

Bywater-Reyes, S., Wilcox, A. C., and Diehl, R. M. (2017). Multiscale influence of woody riparian vegetation on fluvial topography quantified with ground-based and airborne lidar. *J. Geophys. Res.* 122, 1218–1235. doi: 10.1002/2016JF004058

Bywater-Reyes, S., Wilcox, A. C., Stella, J. C., and Lightbody, A. F. (2015). Flow and scour constraints on uprooting of pioneer woody seedlings. *Water Resour. Res.* 51, 9190–9206. doi: 10.1002/2014WR016641

Charru, F., Andreotti, B., and Claudin, P. (2013). Sand ripples and dunes. *Ann. Rev. Fluid Mech.* 45, 469–493. doi: 10.1146/annurev-fluid-011212-140806

Church, M. (2006). Bed material transport and the morphology of alluvial river channels. *Ann. Rev. Earth Planet. Sci.* 34, 325–354. doi: 10.1146/annurev.earth.33.092203.122721

Dean, D. J., and Schmidt, J. C. (2011). The role of feedback mechanisms in historic channel changes of the lower rio grande in the big bend region. *Geomorphology* 126, 333–349. doi: 10.1016/j.geomorph.2010.03.009

Di Tomaso, J. M. (1998). Impact, biology, and ecology of saltcedar (*Tamarix* spp.) in the southwestern United States. *Weed Technol.* 12, 326–336. doi: 10.1017/S0890037X00043906

Diehl, R. M., Merritt, D. M., Wilcox, A. C., and Scott, M. L. (2017a). Applying functional traits to ecogeomorphic processes in riparian ecosystems. *BioScience* 67, 729–743. doi: 10.1093/biosci/bix080

Diehl, R. M., Wilcox, A. C., Stella, J. C., Kui, L., Sklar, L. S., and Lightbody, A. (2017b). Fluvial sediment supply and pioneer woody seedlings as a control on bar-surface topography. *Earth Surf. Process. Landforms* 42, 724–734. doi: 10.1002/esp.4017

Dietrich, W. E., Kirchner, J. W., Ikeda, H., and Iseya, F. (1989). Sediment supply and the development of the coarse surface layer in gravel-bedded rivers. *Nature* 340, 215–217. doi: 10.1038/340215a0

Dietrich, W. E., and Smith, J. D. (1984). Bed load transport in a river meander. *Water Resour. Res.* 20, 1355–1380. doi: 10.1029/WR020i010p01355

Gran, K., and Paola, C. (2001). Riparian vegetation controls on braided stream dynamics. *Water Resour. Res.* 37, 3275–3283. doi: 10.1029/2000WR000203

Gran, K. B., Tal, M., and Wartman, E. D. (2015). Co-evolution of riparian vegetation and channel dynamics in an aggrading braided river system, Mount Pinatubo, Philippines. *Earth Surf. Process. Landforms* 40, 1101–1115. doi: 10.1002/esp.3699

Green, J. C. (2005). Comparison of blockage factors in modelling the resistance of channels containing submerged macrxophytes. *River Res. Appli.* 21, 671–686. doi: 10.1002/rra.854

Griffin, E. R., Kean, J. W., Vincent, K. R., Smith, J. D., and Friedman, J. M. (2005). Modeling effects of bank friction and woody bank vegetation on channel flow and boundary shear stress in the Rio Puerco, New Mexico. *J. Geophys. Res. Earth Surf.* 110:F04023. doi: 10.1029/2005JF000322

Griffin, E. R., Perignon, M. C., Friedman, J. M., and Tucker, G. E. (2014). Effects of woody vegetation on overbank sand transport during a large flood, Rio Puerco, New Mexico. *Geomorphology* 207, 30–50. doi: 10.1016/j.geomorph.2013.10.025

Gurnell, A. (2014). Plants as river system engineers. *Earth Surf. Process. Landforms* 39, 4–25. doi: 10.1002/esp.3397

Hardy, R. J. (2006). Fluvial geomorphology. *Progress Phys. Geogra.* 30, 553–567. doi: 10.1191/0309133306pp498pr

Henderson, F. M. (1963). Stability of alluvial channels. *Transac. Am. Soc. Civil Eng.* 128, 657–686.

Hopkinson, L., and Wynn, T. (2009). Vegetation impacts on near bank flow. *Ecohydrology* 2, 404–418. doi: 10.1002/eco.87

Istanbulluoglu, E., and Bras, R. L. (2005). Vegetation-modulated landscape evolution: effects of vegetation on landscape processes, drainage density, and topography. *J. Geophys. Res.* 110:F02012. doi: 10.1029/2004JF000249

Iwasaki, T., Shimizu, Y., and Kimura, I. (2016). Numerical simulation of bar and bank erosion in a vegetated floodplain: A case study in the Otofuke River. *Adv. Water Resour.* 93, 118–134. doi: 10.1016/j.advwatres.2015.02.001

Johnson, W. C. (1994). Woodland expansion in the Platte River, Nebraska: patterns and causes. *Ecol. Monogra.* 64, 45–84. doi: 10.2307/2937055

Karrenberg, S., Edwards, P. J., and Kollmann, J. (2002). The life history of Salicaceae living in the active zone of floodplains. *Freshwater Biol.* 47, 733–748. doi: 10.1046/j.1365-2427.2002.00894.x

Kean, J. W., and Smith, J. D. (2004). "Flow and boundary shear stress in channels with woody bank vegetation," in *Riparian Vegetation and Fluvial Geomorphology*, eds. S. J. Bennett and A. Simon (Washington, DC: American Geophysical Union), *Water Science and Application* 8, 237–265. doi: 10.1029/008WSA17

Kui, L., Stella, J., Lightbody, A., and Wilcox, A. C. (2014). Ecogeomorphic feedbacks and flood loss of riparian tree seedlings in meandering channel experiments. *Water Resour. Res.* 50, 9366–9384. doi: 10.1002/2014WR015719

Kui, L., and Stella, J. C. (2016). Fluvial sediment burial increases mortality of young riparian trees but induces compensatory growth response in survivors. *Forest Ecol. Manage.* 366, 32–40. doi: 10.1016/j.foreco.2016.02.001

Kui, L., Stella, J. C., Diehl, R. M., Wilcox, A. C., Lightbody, A., and Sklar, L. S. (2019). Can environmental flows moderate riparian invasions? The influence of seedling morphology and density on scour losses in experimental floods. *Freshwater Biol.* 64, 474–484. doi: 10.1111/fwb.13235

Kui, L., Stella, J. C., Shafroth, P. B., House, P. K., and Wilcox, A. C. (2017). The long-term legacy of geomorphic and riparian vegetation feedbacks on the dammed Bill Williams River, Arizona, USA. *Ecohydrology* 10:e1839. doi: 10.1002/eco.1839

Larsen, L. G., Harvey, J. W., and Crimaldi, J. P. (2009). Predicting bed shear stress and its role in sediment dynamics and restoration potential of the Everglades and other vegetated flow systems. *Ecol. Eng.* 35, 1773–1785. doi: 10.1016/j.ecoleng.2009.09.002

Lightbody, A. F., Avener, M. E., and Nepf, H. M. (2008). Observations of short-circuiting flow paths within a free-surface wetland in Augusta, Georgia, U.S.A. *Limnol. Oceanogra.* 53, 1040–1053. doi: 10.4319/lo.2008.53.3.1040

López, F., and García, M. (1998). Open-channel flow through simulated vegetation: Suspended sediment transport modeling. *Water Resour. Res.* 34, 2341–2352. doi: 10.1029/98WR01922

Luhar, M., and Nepf, H. M. (2012). From the blade scale to the reach scale: A characterization of aquatic vegetative drag. *Adv. Water Resour.* 51, 305–316. doi: 10.1016/j.advwatres.2012.02.002

Luna, M. C. M., Parteli, E. J. R., Durán, O., and Herrmann, H. J. (2009). Modeling transverse dunes with vegetation. *Phys. A* 388, 4205–4217. doi: 10.1016/j.physa.2009.06.006

Mahoney, J. M., and Rood, S. B. (1998). Streamflow requirements for cottonwood seedling recruitment: an integrative model. *Wetlands* 18, 634–645. doi: 10.1007/BF03161678

Manners, R., Wilcox, A. C., Kui, L., Lightbody, A., Stella, J., and Sklar, L. (2015). When do plants modify fluvial processes? Plant-hydraulic interactions under variable flow and sediment supply rates. *J. Geophys. Res.* 120, 325–345. doi: 10.1002/2014JF003265

Merritt, D. M. (2013). "Reciprocal relations between riparian vegetation, fluvial landforms, and channel processes," in *Treatise on Geomorphology* Vol. 9, ed E. Wohl (San Diego, CA: Academic Press), 219–243. doi: 10.1016/B978-0-12-374739-6.00239-6

Merritt, D. M., and Poff, N. L. (2010). Shifting dominance of riparian Populus and Tamarix along gradients of flow alteration in western North American rivers. *Ecol. Appl.* 20, 135–152. doi: 10.1890/08-2251.1

Micheli, E. R., and Kirchner, J. W. (2002). Effects of wet meadow riparian vegetation on streambank erosion. 2. Measurements of vegetated bank strength and consequences for failure mechanics. *Earth Surf. Process. Landforms* 27, 687–697. doi: 10.1002/esp.340

Naiman, R. J., and Decamps, H. (1997). The ecology of interfaces: Riparian zones. *Ann. Rev. Ecol. Systemat.* 28, 621–658. doi: 10.1146/annurev.ecolsys.28.1.621

Nepf, H., Rominger, J., and Zong, L. (2013). "Coherent flow structures in vegetated channels," in *Coherent Flow Structures at Earth's Surface*. eds J. G. Venditti, J. L. Best, M. Church and R. J. Hardy (Chichester, UK: John Wiley and Sons, Ltd), 135–147. doi: 10.1002/9781118527221.ch9

Nepf, H. M. (1999). Drag, turbulence, and diffusion in flow through emergent vegetation. *Water Resour. Res.* 35, 479–489. doi: 10.1029/1998WR900069

Nepf, H. M. (2012). Hydrodynamics of vegetated channels. *J. Hydraulic Res.* 50, 262–279. doi: 10.1080/00221686.2012.696559

Neumeier, U., and Ciavola, P. (2004). Flow resistance and associated sedimentary processes in a Spartina maritima salt-marsh. *J. Coastal Res.* 435–447. doi: 10.2112/1551-5036(2004)020[0435:FRAASP]2.0.CO;2

Ortiz, A. C., Ashton, A., and Nepf, H. (2013). Mean and turbulent velocity fields near rigid and flexible plants and the implications for deposition. *J. Geophys. Res.* 118, 2585–2599. doi: 10.1002/2013JF002858

Perucca, E., Camporeale, C., and Ridolfi, L. (2007). Significance of the riparian vegetation dynamics on meandering river morphodynamics. *Water Resour. Res.* 43:W03430. doi: 10.1029/2006WR005234

Platte River Recovery Implementation Program (2006). *Final Platte River Recovery Implementation Program Adaptive Management Plan* (Kearney, NE: Platte River Recovery Implementation Program).

Politti, E., Bertoldi, W., Gurnell, A., and Henshaw, A. (2018). Feedbacks between the riparian Salicaceae and hydrogeomorphic processes: a quantitative review. *Earth-Sci. Rev.* 176, 147–165. doi: 10.1016/j.earscirev.2017.07.018

Rominger, J. T., Lightbody, A. F., and Nepf, H. M. (2010). Effects of added vegetation on sand bar stability and stream hydrodynamics. *J. Hydraulic Eng.* 136, 994–1002. doi: 10.1061/(ASCE)HY.1943-7900.0000215

Rood, S. B., Braatne, J. H., and Hughes, F. M. R. (2003a). Ecophysiology of riparian cottonwoods: stream flow dependency, water relations and restoration. *Tree Physiol.* 23, 1113–1124. doi: 10.1093/treephys/23.16.1113

Rood, S. B., Gourley, C. R., Ammon, E. M., Heki, L. G., Klotz, J. R., Morrison, M. L., et al. (2003b). Flows for floodplain forests: A successful riparian restoration. *BioScience* 53, 647–656. doi: 10.1641/0006-3568(2003)053[0647:FFFFAS]2.0.CO;2

Rood, S. B., Samuelson, G. M., Braatne, J. H., Gourley, C. R., Hughes, F. M. R., and Mahoney, J. M. (2005). Managing river flows to restore floodplain forests. *Front. Ecol. Environ.* 3, 193–201. doi: 10.1890/1540-9295(2005)003[0193:MRFTRF]2.0.CO;2

Sankey, J. B., Ralston, B. E., Grams, P. E., Schmidt, J. C., and Cagney, L. E. (2015). Riparian vegetation, Colorado River, and climate: five decades of spatiotemporal dynamics in the Grand Canyon with river regulation. *J. Geophys. Res.* 120, 1532–1547. doi: 10.1002/2015JG002991

Schmidt, J. C., and Wilcock, P. R. (2008). Metrics for assessing the downstream effects of dams. *Water Resour. Res.* 44:W04404. doi: 10.1029/2006WR005092

Scott, M. L., Friedman, J. M., and Auble, G. T. (1996). Fluvial process and the establishment of bottomland trees. *Geomorphology* 14, 327–339. doi: 10.1016/0169-555X(95)00046-8

Simon, A., and Collison, A. J. (2002). Quantifying the mechanical and hydrologic effects of riparian vegetation on streambank stability. *Earth Surface Process. Landforms* 27, 527–546. doi: 10.1002/esp.325

Solari, L., Van Oorschot, M., Belletti, B., Hendriks, D., Rinaldi, M., and Vargas-Luna, A. (2016). Advances on modelling riparian vegetation—hydromorphology interactions. *River Res. Appl.* 32, 164–178. doi: 10.1002/rra.2910

Stella, J. C., Battles, J. J., McBride, J. R., and Orr, B. K. (2010). Riparian seedling mortality from simulated water table recession, and the design of sustainable flow regimes on regulated rivers. *Restorat. Ecol.* 18, 284–294. doi: 10.1111/j.1526-100X.2010.00651.x

Stella, J. C., Battles, J. J., Orr, B. K., and McBride, J. R. (2006). Synchrony of seed dispersal, hydrology and local climate in a semi-arid river reach in California. *Ecosystems* 9, 1200–1214. doi: 10.1007/s10021-005-0138-y

Stella, J. C., Hayden, M. K., Battles, J. J., Piegav, H., Dufour, S., and Fremier, A. K. (2011). The role of abandoned channels as refugia for sustaining pioneer riparian forest ecosystems. *Ecosystems* 14, 776–790. doi: 10.1007/s10021-011-9446-6

Stromberg, J. C., Lite, S. J., Marler, R., Paradzick, C., Shafroth, P. B., Shorrock, D., et al. (2007). Altered stream-flow regimes and invasive plant species: the Tamarix case. *Global Ecol. Biogeogra.* 16, 381–393. doi: 10.1111/j.1466-8238.2007.00297.x

Tal, M., and Paola, C. (2007). Dynamic single-thread channels maintained by the interaction of flow and vegetation. *Geology* 35, 347–350. doi: 10.1130/G23260A.1

Vargas-Luna, A., Crosato, A., Calvani, G., and Uijttewaal, W. S. J. (2016). Representing plants as rigid cylinders in experiments and models. *Adv. Water Resour.* 93, 205–222. doi: 10.1016/j.advwatres.2015.10.004

Vincent, K., Friedman, J., and Griffin, E. (2009). Erosional consequence of saltcedar control. *Environ. Manage.* 44, 218–227. doi: 10.1007/s00267-009-9314-8

Wahl, T. L. (2000). "Analyzing ADV data using WinADV," in *2000 Joint Conference on Water Resources Engineering and Water Resources Planning and Management,* (Minneapolis). doi: 10.1061/40517(2000)300

Wilcox, A. C., and Shafroth, P. B. (2013). Coupled hydrogeomorphic and woody-seedling responses to controlled flood releases in a dryland river. *Water Resour. Res.* 49, 2843–2860. doi: 10.1002/wrcr.20256

Williams, G. P. (1978). *The case of the shrinking channels—the North Platte and Platte Rivers in Nebraska. U.S. Geological Survey Circular 781.* Arlington, VA: Geological Survey. doi: 10.3133/cir781

Wilson, C. A. M. E., Hoyt, J., and Schnauder, I. (2008). Impact of foliage on the drag force of vegetation in aquatic flows. *J. Hydraulic Eng.* 134, 885–891. doi: 10.1061/(ASCE)0733-9429(2008)134:7(885)

Wu, W., Shields, F. D., Bennett, S. J., and Wang, S. S. (2005). A depth-averaged two-dimensional model for flow, sediment transport, and bed topography in curved channels with riparian vegetation. *Water Resour. Res.* 41:W03015. doi: 10.1029/2004WR003730

Yager, E. M., and Schmeeckle, M. W. (2013). The influence of vegetation on turbulence and bed load transport. *J. Geophys. Res.* 118, 1585–1601. doi: 10.1002/jgrf.20085

Conflict of Interest Statement: The authors declare that the research was conducted in the absence of any commercial or financial relationships that could be construed as a potential conflict of interest.